

# Dynamic centrifuge modelling facilities at the University of Dundee and their application to studying seismic case histories

A.J. Brennan & J.A. Knappett

*University of Dundee, UK*

D. Bertalot

*D'Appolonia S.p.A., Genoa, Italy (formerly University of Dundee, UK)*

M. Loli & I. Anastasopoulos

*National Technical University of Athens, Greece*

**ABSTRACT:** This paper has the twin aim of presenting the new Actidyn Q67-2 shaker installed at the University of Dundee, with consideration of motion replication and repeatability, and also to demonstrate one particular advantage of the “real earthquake” motion capability in validating and enhancing learning from earthquake case histories. Case histories of liquefaction-induced settlements from the Maule earthquake in Chile in 2010 and soil structure interaction from the Kobe earthquake in Japan in 1995 are presented.

## 1 INTRODUCTION

Case histories are of great benefit to the study of earthquake related engineering risks, as each major earthquake event serves to test our understanding of seismic system performance. Many lessons are learned by studying case histories, and field investigation after major earthquakes is an important factor in the reduction of seismic risk. However, each case history occurs due to a particular combination of circumstances. Soil conditions, motion amplitude/duration/frequency content, topography, existing infrastructure, fault characteristics and epicentral distance (e.g.) all contribute to make each seismic event of the past different from the seismic events of the future, the understanding of which is our ultimate goal. Therefore, for a number of years, physical modelling has played a role in furthering understanding by producing idealized prototype case histories in which the influence of various factors can be examined in isolation. When geotechnical systems are under scrutiny, the centrifuge has become a standard tool due to its reproduction of full scale stresses in small scale models.

Dynamic physical modelling has consequently developed significantly over the past 35 years. Early narrow band systems, capable of motions with limited control and a limited range of shaking are reviewed by Derkx et al. (2006). The development of servo-hydraulic shakers (e.g. Chazelas et al., 2008; Madabhushi et al., 2012) has permitted more broad banded motions to be realised, and the majority of new installations over the past decade have been of this type.

Such complicated shakers giving such a range of choice of motion to the modeller has changed the

range of questions that may be asked of a centrifuge model, but also introduced a potentially large number of variables, as the amplitude, frequency spectrum and duration of applied motion(s) must be carefully chosen to achieve a desired result. This is not a decision to be taken without due consideration, and has no universal answer. For example, Mason et al. (2010) describe testing over a broad suite of motions to cover a range of possibilities in line with US building code specifications of at least five motions although it is still common to apply simple sinusoidal motions (e.g. Kamai and Boulanger, 2010) or to use a motion that has been shown to be reproduced on the available system (e.g. Mason et al., 2010). The point must be that now motions may be more carefully designed and controlled than motion selection must be justified with regard to the desired outcome or learning.

This paper therefore has the twin aim of presenting the new Actidyn Q67-2 shaker installed at the University of Dundee, with consideration of motion repeatability, and also to demonstrate one particular advantage of the “real earthquake” motion capability in validating and enhancing learning from earthquake case histories.

## 2 DUNDEE SHAKER

The Dundee shaker is Actidyn model Q67-2, a device based on that proposed by Perdriat et al. (2002) (2002) and implemented at C-CORE and IFFSTAR (formerly LCPC) (Chazelas et al., 2008). Key features of the device are listed below.

## 2.1 Mechanical Features

Necessitated by the reduced space available on the Dundee centrifuge, where the permanent addition of components would have compromised the ability to test the larger packages used previously, the shaker features an integral actuator-basket design. Thus the centrifuge may be returned to its previous configuration by removing the entire swinging basket and replacing it with the “static” basket. The removable actuator enables pre-existing packages to still be tested, and the integral design optimises turnaround between static and dynamic tests. The integral basket arrangement is shown mounted on the centrifuge in Figure 1. In this image, the payload is not present, but will sit in the position marked and subsequently enclosed by a wall in the place of the open end of the package.

A further advantage of the integral design is enabling the pressure accumulators to be located as close as possible to the actuators, minimizing in-pipe oil travel. This does, however, necessitate repeated transfer of oil to and away from the package during flight. Thus 60 kg of oil is added, then removed from the centrifuge payload in every two or three minute period during operation. As the Dundee centrifuge is statically balanced prior to spinning and is unable to respond to changes in package mass, this causes a fluctuation in the centrifuge out-of-balance according to Equation 1, in which  $m$  is mass of oil and  $Ng$  is the centrifuge acceleration at the oil location (below the package) in  $m/s^2$ . In tests at 50g, therefore, the expected  $\pm 15$  kN out of balance has been recorded. This is much less than the design maximum out-of-balance (warning alarm triggered at  $\pm 45$  kN, automatic shutdown at  $\pm 55$  kN) but the cyclic nature of this loading mean caution must be taken in the future with regard to centrifuge component fatigue.

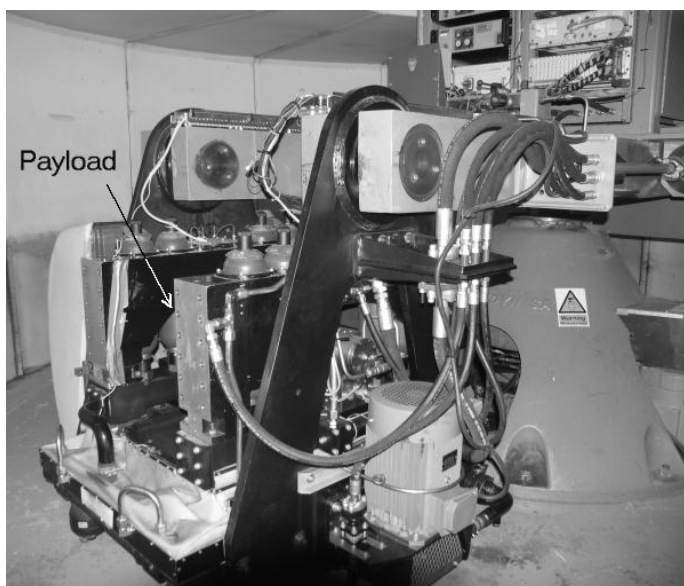


Figure 1. Swinging basket with integral shaking actuator.

Table 1. Selected specifications for Dundee shaker

Payload mass	400 kg
Payload footprint	0.8 m x 0.4 m
Payload height	0.6 m
Peak operational g level	80g
Displacement limits	2.5 mm
Velocity limit	0.75 m/s
Acceleration limit	40g*

\*Frequency dependent (see Figure 2)

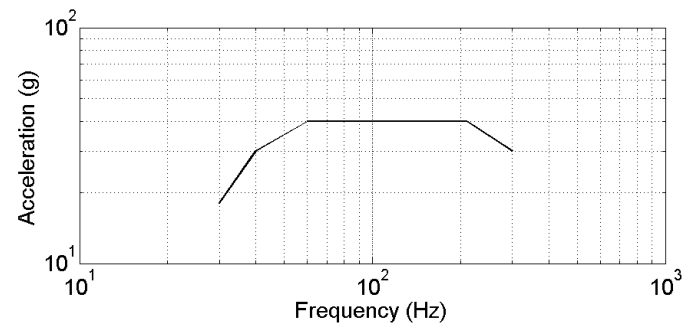


Figure 2. Operating map of peak acceleration as a function of frequency.

Dynamic balancing of the shaking payload is also important. The package is surrounded by a counterweight that moves in antiphase to the payload and hence minimises parasitic reaction accelerations that may be transmitted into the centrifuge arm (Perdriat et al., 2002).

The design also features two pressurized back to back oil film bearings reduce base friction and to provide adequate base stiffness against bending and pitching.

Specifications of the shaker are given in Table 1. Note that the displacement acts as the most stringent limit on low frequency response, and acceleration at high frequency. It is therefore beneficial to consider the response in terms of an operating map of peak accelerations as shown in Figure 2.

## 2.2 Motion Features

Motion is controlled by a SignalStar Matrix controller produced by Data Physics Corp. This provides the repeatability in reproducing desired motions. The principle is that before a test series, the motion must be calibrated on a dummy package, which can be a solid block of appropriate mass and stiffness but is in practice an exact replica of the model to be tested in the series. This has been found to provide the additional advantage of allowing trainee researchers to practice model making and centrifuge set up. Also, if instrumented, some dynamic measurements can be taken during the calibration which can be used for, e.g., examination of the evolution of stress-strain loops at different strain levels, or an appraisal of the

amount of pore pressure that may be generated by repeated seismic loading.

Once the dummy payload is set up and taken to the required g level, a series of initial random burst pre-test motions are implemented in order to identify a transfer function for the mechanical system. Having established this, the controller calculates an input signal that would be most likely to achieve the desired motion in the model. A reduced amplitude version of this shake is triggered, following which the controller recalculates an input signal. When the error between target and achieved motion has reduced to a small level, the amplitude of the target motion is increased and the process repeated until the full-scale version of the target motion has been satisfactorily reproduced on the package. This motion is then noted. For the rest of the test series, this motion may then be recalled and applied directly onto new models, eliminating the need to calibrate for every test. Example data from a calibration is shown in Figures 3 and 4, in which successive events are triggered with successive improvement in the discrepancy between target acceleration and that achieved. Data is taken from the calibration of the Maule earthquake (see below) with amplitudes reduced by 12 dB, chosen only because of the large quantity of data recorded at this stage. This is shown in Figure 3 in the time domain of acceleration measured in three (non consecutive) shakes, together with an error function, calculated as the difference between target motion and the measured value. The frequency distribution of these quantities for the first and last event is shown in Figure 4.

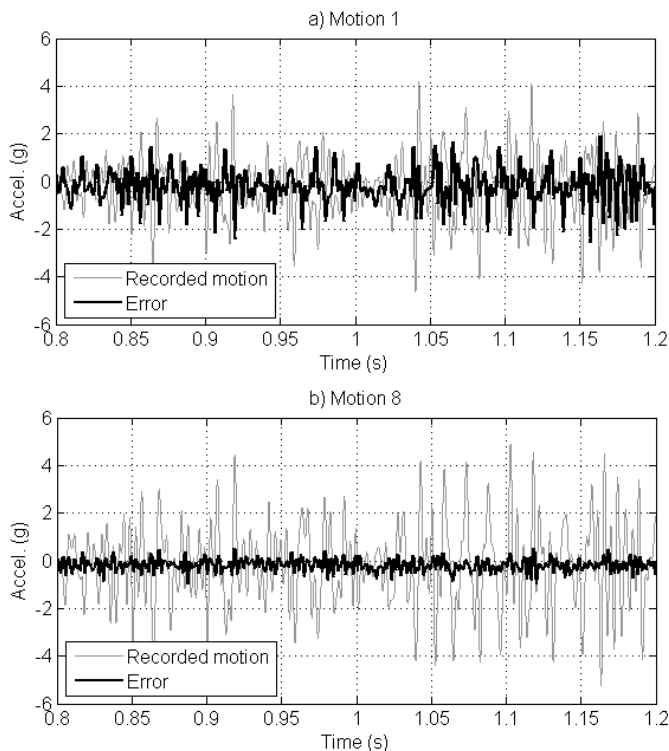


Figure 3. Motion evolution during calibration (time domain).

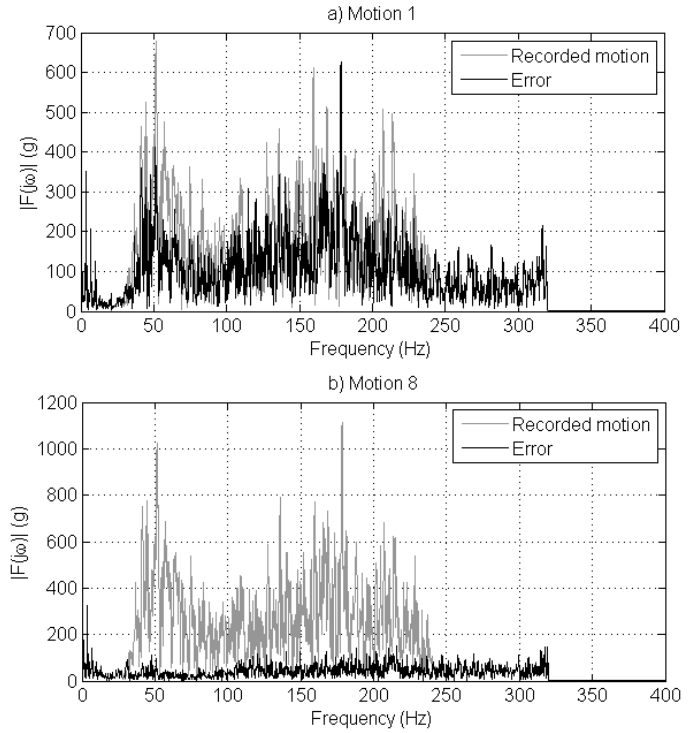


Figure 4. Motions during calibration (frequency domain).

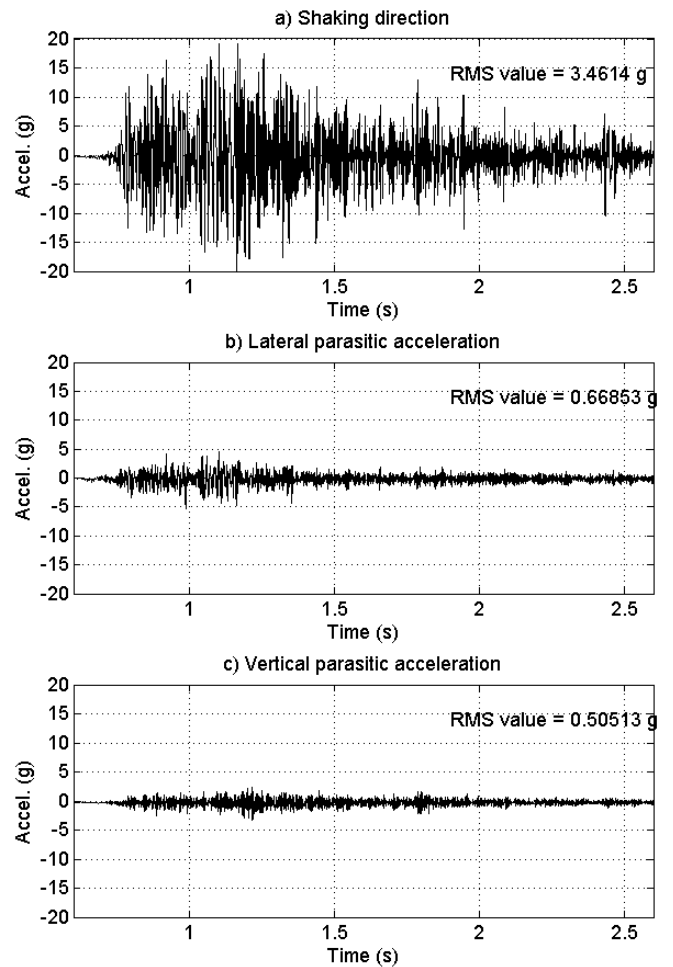


Figure 5. Example measured acceleration in a) desired direction, b) lateral direction and c) vertical direction.

Both Figures 3a and 4a show that the error signal of the initial guess is of a comparable amplitude to

the motion produced. It is worth noting that were the system not able to train itself to improve the target matching, then these would represent the final error achieved. However, by allowing the system to refine its motion then the motion improves, and Figures 3b and 4b show that in this case after eight events then the error has reduced to almost negligible levels.

The calibration process enables the displacements, velocities and accelerations of the shaking to be monitored in order to ensure that the system limits are not exceeded. Whilst these are calculated in advance, safety dictates that is good practice to monitor these values during calibration.

Spurious accelerations in the “non-shaking” directions (lateral and vertical) are not controlled but are monitored. These have been specified to be less than a fraction of the root mean square (RMS) desired target acceleration, being 20% in the vertical case and 10% in the lateral direction. Figure 4 shows these values as measured at the end of the calibration of the Maule shake. Both off-axis accelerations are much smaller than the shaking in the desired direction, although the RMS amplitude of the lateral acceleration is higher than intended at 19% of intended shaking RMS amplitude.

### 3 MAULE EARTHQUAKE, CHILE, 2010

The  $M_w = 8.8$  Maule earthquake hit Chile on the February 27th 2010 at 6.34 am (UTC time). The hypocentre was at a depth of 30.1 km and was located offshore the coastal town of Cobquecura, around 100 km north of the city of Concepción, at latitude  $36.29^\circ\text{S}$  and longitude  $73.239^\circ\text{W}$ . The city of Concepción and its surroundings were among the locations most affected by liquefaction. Several cases of liquefaction induced ground failures were observed in the Concepción area ranging from lateral spreading of sloping ground and bridge abutments to building settlement and tilting and uplift of buried structures. As part of a study on the liquefaction-induced settlement of shallow foundations, 23 buildings were surveyed following the event. A full description of the survey is presented by Bertalot et al. (2012).

This field data proved a valuable addition to the existing set of field data, and one aspect of interest was that the bearing pressure imposed by the structures, which had previously not been considered as a variable in settlement estimation, was shown to be a significant influence. Figure 6 shows normalized settlements from the Maule case, together with literature data from Niigata (reported by Yoshimi and Tokimatsu, 1977), and Luzon (Adachi et al., 1992 and Acacio et al., 2001). It was clear from the full data set that increasing bearing pressure led to increased settlements, but it also appeared that for very high bearing pressures, this trend was reversed. In order to determine whether this was a genuine effect

or an anomaly of the field data available, a series of centrifuge tests were performed.

In these tests, four square footings of equal dimensions ( $B = 55$  mm model scale) but different bearing pressures were installed in liquefiable sand of given thickness. In line with the field cases, the motion chosen for the centrifuge tests was the nearest record to the Maule cases, the San Pedro station (Figure 5a). Note that the purpose in this case was not to reproduce the exact field data but to eliminate one of the variables when comparing between the centrifuge and the field data. Testing was carried out at 50 g centrifuge acceleration. Full test details are provided by Bertalot, (2013) and by Bertalot and Brennan (2014).

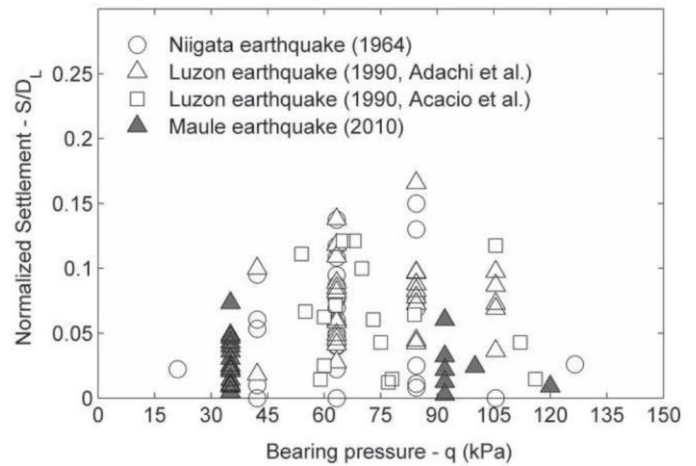


Figure 6. Settlement as a function of structure bearing pressure from field studies.

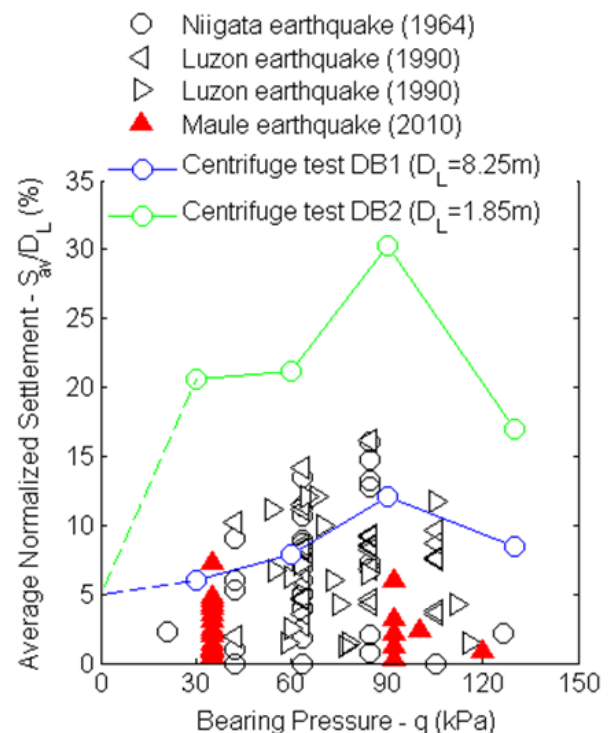


Figure 7. Comparison between centrifuge and field trends.

Figure 7 shows how these four footings of different bearing pressure settled on liquefiable layers of thickness  $D_L = 8,25$  m and 1.85 m prototype scale. The principal point to note from this figure is that the observed field trend, of settlements being a strong function of applied bearing pressure is also demonstrated by the centrifuge model. It must also be noted that the trend is identical to the field cases, in that settlement increases with increasing bearing pressure as would be expected, counter-intuitively settlements for very high bearing pressure footings ( $> 90$  kPa in this case) are inhibited. It is believed that this is related to the stress distribution beneath such footings (Bertalot and Brennan, 2014).

#### 4 KOBE EARTHQUAKE, JAPAN 1995

This case is based on the well-known structural collapse of the Hanshin Expressway during the 1995 Kobe earthquake. This structure was a very long highway bridge supported at regular intervals by single circular reinforced concrete (RC) columns. This structural failure has been one of the key drivers behind the recent development of ‘rocking isolation’ design concepts, in which the foundation is designed to yield at a lower critical acceleration compared to the structure, thereby preventing catastrophic structural failure, albeit at the expense of (significant) foundation settlement.

The aim in this project was not to investigate the specific structural design of the Hanshin Expressway, but to examine more generically the collapse behaviour and soil-structure interaction (SSI) of single-pier reinforced concrete bridge structures that have been aseismically designed (i.e. that should be nominally resistant to a design level of shaking).

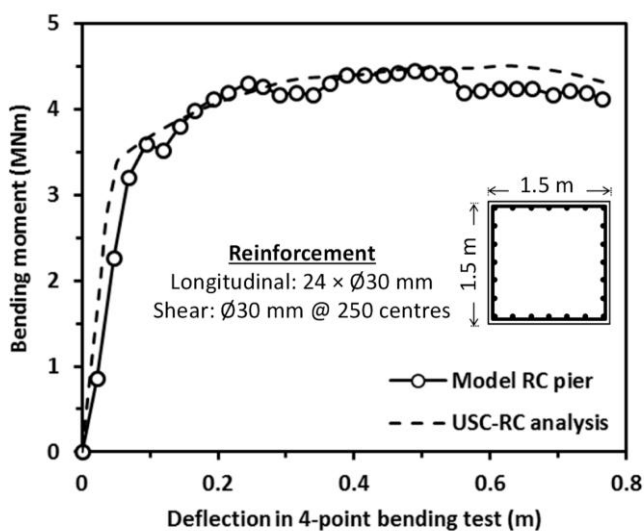


Figure 8. Structural properties of model RC bridge pier, bending properties from four-point bending test. All values at prototype scale.

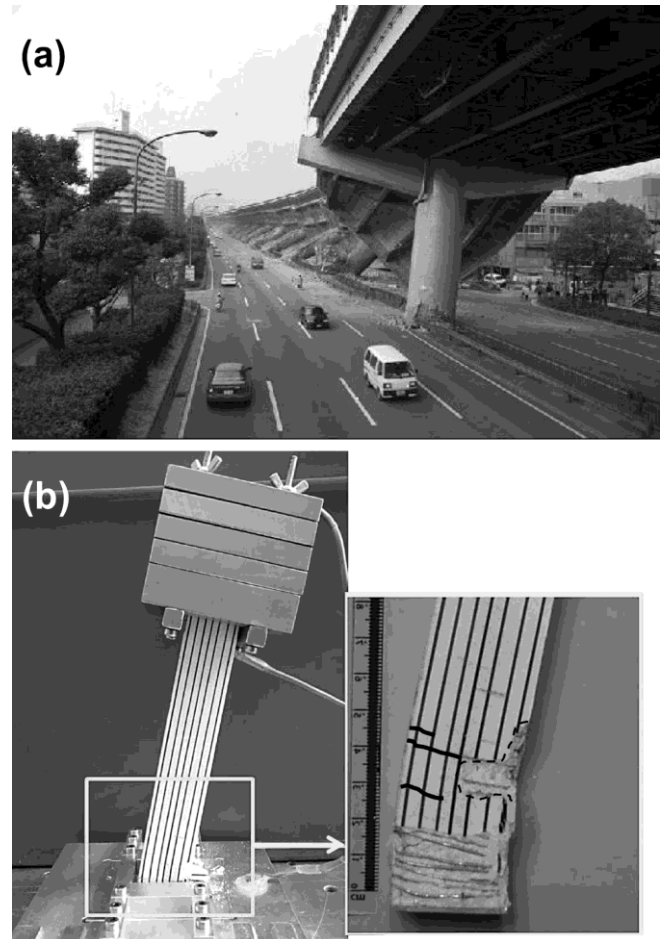


Figure 9. (a) Damage to Hanshin Expressway following 1995 Kobe earthquake; (b) damage to model RC bridge pier model in centrifuge test.

This project also highlights another piece of complementary new centrifuge technology recently developed at the University of Dundee, namely small scale reinforced concrete (Knappett et al. 2011).

The pier had the reinforcement layout and moment capacity shown in Figure 8, which provided a close match to the behaviour determined from a standard reinforced concrete section analysis programme (USC-RC). In the interests of brevity, details of the model layout and soil properties are not given here, but may be found in Loli et al. (2014). The suitability of the model concrete for producing correctly scaled behaviour in a centrifuge model test is explored further in Al-Defae and Knappett (2014).

Figure 9a shows damage observed to one of the bridge piers of the Hanshin Expressway, indicating significant rotation of the column due to damage induced at its base. Figure 9b shows a similar image of the model bridge pier from the centrifuge test. The model pier has exhibited classic damage patterns at the base where the bending moments and shear forces are highest, namely tension cracking on one side and compressive spalling on the opposite side, resulting in permanent rotation of the pier and consequent drift of the bridge deck. The pier was actually subjected to five different earthquake motions of increasing magnitude and intensity during the test; response spectra for these motions for nom-

inal 5% structural damping are shown in Figure 10. The order of the motions (in terms of increasing expected structural damage based on preliminary 3-D non-linear FE analyses) was Aegion, Lefkada, L'Aquila, Northridge, Kobe. Onboard video capture revealed that the damage shown in Figure 9b occurred during the Kobe earthquake; from Figure 10 the natural period of the bridge structure increases as the elastic bending stiffness reduces (as yield is approached). It can be seen that the Kobe motion is particularly damaging to a structure such as this, resulting in high spectral accelerations (and therefore high induced shear forces and bending moments).

The ability to accurately replicate such a wide range of motions, combined with improvements in modelling structural materials more realistically, allows for greater insight into seismic SSI problems within a geotechnical centrifuge.

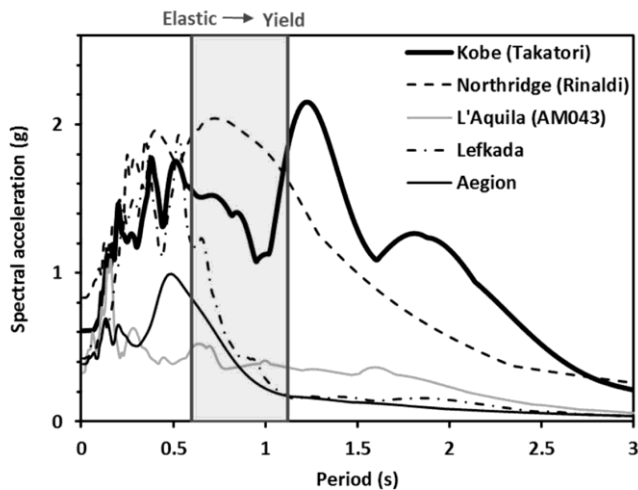


Figure 10. Response spectra (plotted for nominal 5% structural damping) for historical demand motions used in the centrifuge testing programme.

## 5 SUMMARY

This paper has reviewed the new earthquake shaker installed on the University of Dundee geotechnical centrifuge, together with related infrastructure. Now that such devices are becoming increasingly common, the variable of input motion has been opened up for researchers. Selection of input motion is clearly key to asking the right question of a dynamic centrifuge model. Review of two projects recently carried out at Dundee has exemplified one strategy, namely the use of previously recorded strong motion in order to better understand observed damage during that particular event and hence complement field reconnaissance.

## REFERENCES

- Acacio, A., Kobayashi, Y., Towhata, I., Bautista, R. T. and Ishihara, K. 2001. Subsidence of building foundation resting upon liquefied subsoil: case studies and assessment. *Soils and Foundation*, 41(6), 111-128.
- Adachi, T., Iwai, S., Yasui, M. and Sato, Y. 1992. Settlement and Inclination of Reinforced-Concrete Buildings in Daguapan-City due to Liquefaction during the 1990 Philippine Earthquake. Proceedings of the 10th World Conference on Earthquake Engineering, 1, 147-152.
- Al-Defae, A.H. & Knappett, J.A. 2014. Stiffness matching of model reinforced concrete for centrifuge modelling of soil-structure interaction. Proc. 8th Int. Conf. on Physical Modelling in Geotechnics ICPMG '14, Perth, Australia.
- Bertalot, D. 2013. Seismic behaviour of shallow foundations on layered liquefiable soils. PhD thesis, University of Dundee, UK
- Bertalot, D., Brennan, A.J. & Villalobos, F.A. 2012. Influence of bearing pressure on liquefaction-induced settlement of shallow foundations *Géotechnique* 63(5): 391-399. doi: 10.1680/geot.11.P.040
- Bertalot, D. & Brennan, A.J. 2014. Influence of initial shear stress on earthquake induced excess pore pressure generation beneath shallow foundations. *Géotechnique (under review)*.
- Chazelas, J.L., Escoffier, S., Garnier, J., Thorel, L. & Rault, G. 2008. Original technologies for proven performance for the new LCPC earthquake simulator. *Bulletin of Earthquake Engineering* 6(4): 723-728. doi: 10.1007/s10518-008-9096-z
- Derksz, F., Thorel, L., Chazelas, J.L., Escoffier, S., Rault, G., Buttigieg, S., Cottineau, L.M. & Garnier, J. 2006. Dynamic tests and simulation of earthquakes in the LCPC's centrifuge. In C.W.W. Ng, L.M. Zhang and Y.H. Wang (eds.), *Proc. 6<sup>th</sup> Int. Conf. on Physical Modelling in Geotechnics (ICPMG 06)*. 181-186.
- Kamai, R. & Boulanger, R.W. 2010. Characterizing localization processes during liquefaction using inverse analysis of instrumentation arrays. In Y.H. Hatzor, J. Sulem and I. Vardoulakis (eds.), *Meso-Scale Shear Physics in Earthquake and Landslide Mechanics*: 219-238. CRC Press.
- Knappett, J.A., Reid, C., Kinmond, S. and O'Reilly, K. 2011. Small scale modelling of reinforced concrete structural elements for use in a geotechnical centrifuge. *Journal of Structural Engineering*, ASCE, 137(11): 1263-1271.
- Loli, M., Knappett, J.A., Brown, M.J. and Anastopoulos, I. 2014. Use of Ricker wavelet ground motions as an alternative to push-over testing. Proc. 8th Int. Conf. on Physical Modelling in Geotechnics ICPMG '14, Perth, Australia.
- Madabhushi, S.P.G., Haigh, S.K., Houghton, N.E. & Gould, E. 2012. Development of a servo-hydraulic earthquake actuator for the Cambridge Turner beam centrifuge. *International Journal of Physical Modelling in Geotechnics* 12(2): 77-88. doi: 10.1680/ijpmg.11.00013
- Mason, H.B., Bray, J.D., Kutter, B.L., Wilson, D.W. & Choy, B.Y. 2010. Earthquake motion selection and calibration for use in a geotechnical centrifuge. In S. Springman, J. Laue and L. Seward (eds.), *Physical Modelling in Geotechnics ICPMG 2010*: 361-366. CRC Press.
- Perdriat, J., Phillips, R., Nicolas Font, J. & Hutin, C. 2002. Dynamically balanced broad frequency earthquake simulation system. In R. Phillips, P.J. Guo & R. Popescu (eds.), *Proc. 5<sup>th</sup> Int. Conf. on Physical Modelling in Geotechnics (ICPMG 02)*. 169-174.
- Yoshimi, Y. and Tokimatsu, K. 1977. Settlement of buildings on saturated sands during earthquakes. *Soils and Foundations*, 17(1), 23-28